

Electron-phonon interactions in bct white tin

V RAMAMURTHY

Department of Physics, Indian Institute of Technology, New Delhi 110016, India

MS received 2 December 1985

Abstract. The electron-phonon interactions are evaluated exactly over the actual shape of the atomic polyhedron as well as the lattice polyhedron of diatomic white tin by making use of simple coordinate axes transformations and crystal symmetry. It is shown that the expressions for the interference factor, $S(\mathbf{q}, t)$ of the atomic polyhedron are complex while those for the lattice polyhedron are real and the reciprocal lattice vectors derived from the former do not correspond to those derived either from the latter or from x-ray structure factors. By comparing these expressions with each other as well as with those obtained by approximating these polyhedra by an ellipsoid of equivalent volume, apparent differences between the interference factors of atomic and lattice polyhedra, consequent ambiguity regarding the shape and size of the first Brillouin zone of white tin, validity of the Wigner-Seitz approximation for a diatomic lattice and the manner in which the electron-phonon interactions contribute to acoustical and optical modes of vibration are discussed.

Keywords. Electron-phonon interactions; interference factor; coordinate axes transformation; atomic polyhedron; Brillouin zone; bct white tin.

PACS No. 63-20

1. Introduction

The electron-phonon interactions which manifest themselves whenever the energies of the conduction electrons are perturbed, should be evaluated by averaging the thermal motion of the ion over the actual shape of the atomic polyhedron without approximating it by a sphere or an ellipsoid of equivalent volume. There is no other means of obtaining the form factors and the interference factors which are consistent with the lattice symmetry especially because the Wigner-Seitz approximation makes the energy of the electron a function of the atomic volume only but not of the type of the crystal structure (Wilson 1954). In addition, the amplitude of thermal motion of a lattice atom differs from that of a basis atom in a diatomic solid and it is absolutely essential to distinguish between their respective contributions to the interference factor, $S(\mathbf{q})$ in order to restore the translational symmetry to the optical modes of vibration. Keeping these objectives in mind, Ramamurthy (1978) showed that this sum could be evaluated exactly in the case of cubic structures by making use of their lattice symmetry and the apparently different expressions obtained by Bross and Bohn (1967), Sharan *et al* (1973) and Ashokkumar (1973) are just one or the other of the several alternative (but equivalent) ways of writing down the interference factor, $S(\mathbf{q})$. Further, the same procedure has been adopted by Ramamurthy in deducing the interference factors for monatomic tetragonal structures (Ramamurthy 1979, hereinafter referred to as I) and polyatomic close packed structures (Ramamurthy 1985) and all these expressions invariably reduce to zero at a reciprocal lattice vector, $\mathbf{g} \neq 0$.

The cubic close-packed structures could be viewed either as a monatomic lattice or as a triatomic lattice by referring it, respectively, to cubic or orthorhombic co-ordinate axes, the x , y and z axes of the latter being oriented along $[\bar{1}10]$, $[\bar{1}\bar{1}2]$ and $[111]$ directions of the former. However, it was observed that the set of reciprocal lattice vectors associated with this atomic arrangement differs significantly from one axes to another, although the shape and size of the atomic polyhedron remain unaltered. Consequently, the Brillouin zone of the monatomic lattice is compatible with the atomic polyhedron whereas that of the triatomic lattice is not. Besides the latter is reduced in size by the introduction of optical modes of vibration. It appears as though the basis atoms of a polyatomic lattice alter the shape and size of the Brillouin zone and hence destroy its compatibility with the atomic polyhedron. On the other hand, contributions from the umklapp processes to different modes of vibration should be summed over a set of reciprocal lattice vectors which is consistent with the latter. It is therefore necessary to understand the dependence of the shape and size of the Brillouin zone on the number of atoms associated with a lattice point and the manner in which it is linked with the reciprocal lattice. For this purpose, the exact evaluation of the interference factors associated with the atomic polyhedron as well as the lattice polyhedron, which is the Wigner-Seitz cell around a lattice point, of bct white tin is described in this paper. The correct link between the Brillouin zone of diatomic bct lattice and its polyhedra is established by comparing the reciprocal lattice vectors which reduce either of the expressions for $S(\mathbf{q})$ to zero with those obtained from x-ray structure factors.

2. Theory

When the band structure effects and the exchange as well as the correlation effects associated with the conduction electrons present in the atomic polyhedron are taken into account through appropriate effective mass and screening function (Ramamurthy and Rajendraprasad 1982), respectively and the effect of the thermal motion of the ion, represented by the phonon wavevector, \mathbf{q} , is evaluated exactly over these electrons, treating them as free, the interference factor, $S(\mathbf{q})$ is given by

$$S(\mathbf{q}) = \int_{\Omega} \exp(i\mathbf{q} \cdot \mathbf{r}) d\Omega / \Omega, \quad (1)$$

where Ω is the volume of the atomic polyhedron. This expression could be reduced, by making use of some vector identities involving ∇ (see equation (2) in I) and Gauss' divergence theorem, to the following forms:

$$S_2(\mathbf{q}) = \frac{(\sigma_x + \sigma_y + \sigma_z)}{\Omega(q_x + q_y + q_z)}, \quad (2a)$$

$$S_3(\mathbf{q}) = \frac{(q_x \sigma_x + q_y \sigma_y + q_z \sigma_z)}{\Omega(q_x^2 + q_y^2 + q_z^2)}. \quad (2b)$$

Here σ_x , σ_y and σ_z are the Cartesian components of σ defined by

$$\sigma = \frac{1}{i} \int_s \exp(i\mathbf{q} \cdot \mathbf{r}) ds, \quad (3)$$

where the integration is over the surface of the atomic polyhedron and hence has to be evaluated separately for each crystal structure. This integral is evaluated in the case of diatomic white tin by exploiting its lattice symmetry in the next section.

3. Evaluation of the interference factors

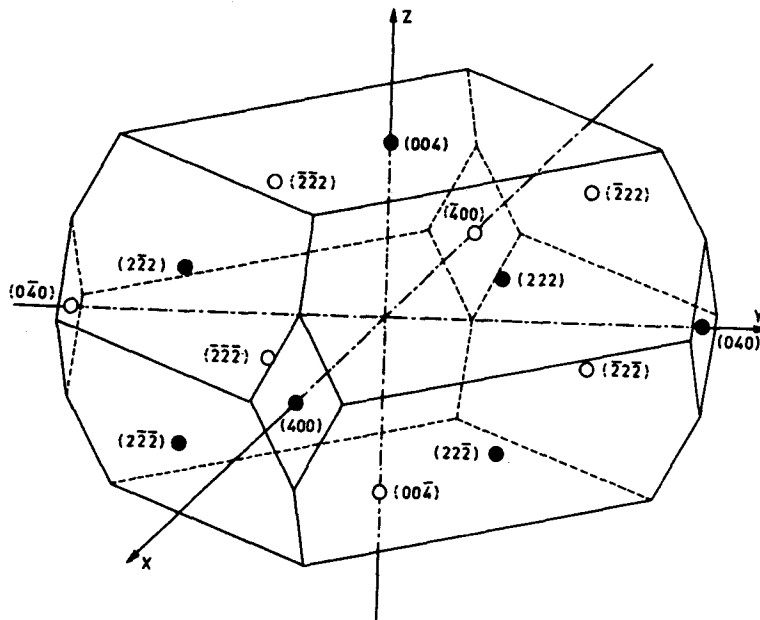
3.1 Lattice polyhedron of diatomic white tin

The atomic positions of white tin are represented by two identical, interpenetrating bct lattices with axial ratio, $t < 1$. One of these lattices is generated from the other by a basis vector, $\mathbf{b} = (a/4)(2\hat{i} + t\hat{k})$ where a and c are the lattice parameters, $t = c/a$ and $\hat{i}, \hat{j}, \hat{k}$ are the unit vectors along x, y, z directions. The lattice polyhedron which is formed by perpendicular planes bisecting the lines joining an atom with its first, second and third nearest neighbour atoms located on the same lattice (the intervening basis atoms located on the other lattice being ignored) is shown in figure 1(a). It is a tetrakaidecahedron consisting of a pair of (004) square faces and two pairs of ((400)) rhombic faces of sides $(a/4)(2 - t^2)\sqrt{2}$ and $(c/4)(1 + t^2)^{1/2}$ respectively, as well as four pairs of irregular ((222)) hexagonal faces. Each of the former two has one side common with the latter. Each pair of the latter contributes to all components of σ whereas that of the former contributes to one or the other component. Nevertheless the symmetry associated with the lattice polyhedron reduces the evaluation of σ to that of contributions from a pair of hexagonal faces and rhombic faces to σ_x and that from the square faces to σ_z . Since this polyhedron is identical in shape and size with the atomic polyhedron of monatomic bct lattice with $t < 1$, described in I, except for the fact that the Miller indices of the faces of the former are obtained by doubling those of the latter, the evaluation of the integral, in either case, yields the same expressions for σ_x, σ_y and σ_z as those given in §3.2 of I, but these are not reproduced here.

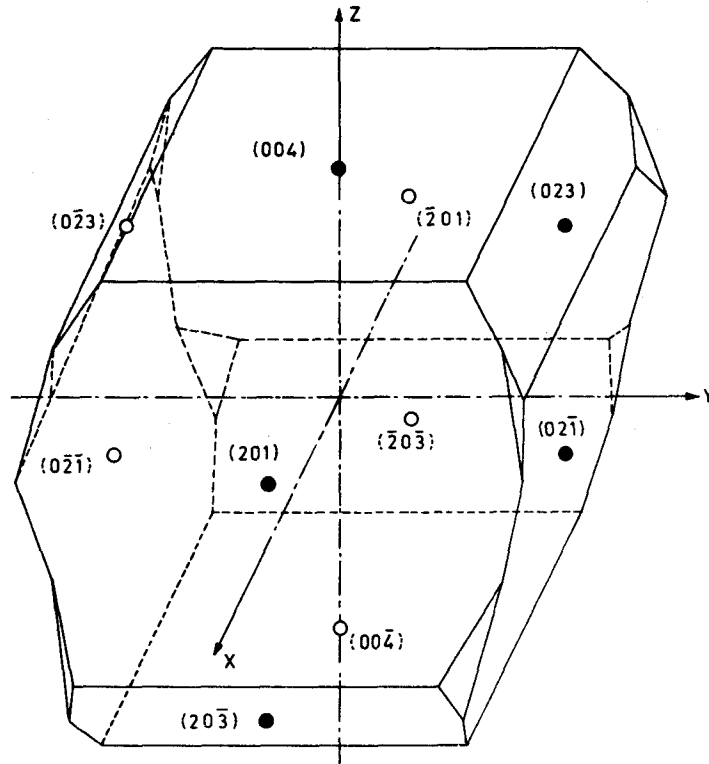
3.2 Atomic polyhedron of diatomic white tin

The atomic polyhedron which is formed by perpendicular planes bisecting the lines joining an atom of white tin with its first, second, third and fourth nearest neighbour atoms (without bothering about the lattice on which they are located) is shown in figure 1(b). It is an octakaidecahedron consisting of a pair of (004) square faces and four pairs of ((222)) isosceles triangular faces of sides $a(4 - 3t^2)/8$ and $c(4 + 10t^2)^{1/2}/16$, respectively, as well as incomplete sets of four ((201)) irregular decagonal faces and four ((023)) irregular hexagonal faces which intersect either x or y axis at $\pm (a/4)$ where a and c are the lattice parameters and $t = c/a$. All these faces contribute to σ_z , decagonal and hexagonal faces contribute either to σ_x or σ_y , whereas the square and triangular faces contribute to neither and both components, respectively. However, the symmetry associated with the atomic polyhedron reduces the evaluation of σ to that of contributions from a pair of square faces, two pairs of triangular faces, a decagonal face and a hexagonal face to σ_z . Since the square faces are perpendicular to z axis, their contribution to σ_z could be written as

$$\sigma_z(004) = \left[\frac{\exp(iq_z z)}{i} \right]_{-c/2}^{c/2} \int_{-d'}^{d'} \int_{-d'}^{d'} \exp(iq_x x) \exp(iq_y y) ds_z, \quad (4)$$



(a)



(b)

Figure 1. (a) Lattice polyhedron and (b) atomic polyhedron of diatomic white tin referred to tetragonal co-ordinate axes. ●, ○ and triple integers denote the centre and Miller indices of each face. (004) and ((222)) faces are common to both polyhedra.

where $d' = a(4 - 3t^2)/16$. This integral is evaluated to obtain

$$\sigma_z(004) = 8 \sin(q_z c/2) \sin(q_x d') \sin(q_y d') / q_x q_y. \quad (5)$$

Further, the co-ordinate axes transformation

$$Z = \frac{(x + y + tz)}{\sqrt{(2 + t^2)}}; \quad X = \frac{(y - x)}{\sqrt{2}} \quad \text{and} \quad Y = \frac{(t(2z/t - x - y))}{\sqrt{2(2 + t^2)}} \quad (6)$$

with positive and negative x, y respectively orients (222) and $(\bar{2}\bar{2}\bar{2})$ pairs of triangular faces perpendicular to Z axis. Hence their contributions could be expressed as

$$\begin{aligned} \sigma_z(222) = & \left[\frac{\exp[i(tq_z + q_x + q_y)Z]}{i} \right]_{-a/4}^{a/4} \\ & \times \int_e^{e'} \int_{-e}^e \exp[i(q_y - q_x)X] \exp[i(2q'_z - q_x - q_y)Y] ds_z \quad (7) \end{aligned}$$

and

$$\begin{aligned} \sigma_z(\bar{2}\bar{2}\bar{2}) = & \left[\frac{\exp[i(tq_z - q_x - q_y)Z]}{i} \right]_{-a/4}^{a/4} \\ & \times \int_{-e}^{-e'} \int_{-e}^e \exp[-i(q_y - q_x)X] \exp[i(2q'_z + q_x + q_y)Y] ds_z, \quad (8) \end{aligned}$$

where $e = at^2/16$, $e' = 3e$ and $q'_z = (q_z/t)$. The evaluation of these integrals yields

$$\begin{aligned} \sigma_z(222) = & \left[\frac{4 \exp[i(tq_z + q_x + q_y)a/4]}{it(2q'_z - 3q_x + q_y)(2q'_z + q_x - 3q_y)} \left\{ \exp[i(q_y - q_x)e'] \right. \right. \\ & - \exp[i(q_y - q_x)e] \left(\cos[(2q'_z - q_x - q_y)e] \right. \\ & \left. \left. + \frac{2i(q_y - q_x) \sin[(2q'_z - q_x - q_y)e]}{(2q'_z - q_x - q_y)} \right) \right\} \\ & \left. + (\text{complex conjugate}) \right] \quad (9) \end{aligned}$$

and

$$\begin{aligned} \sigma_z(\bar{2}\bar{2}\bar{2}) = & \left[\frac{4 \exp[i(tq_z - q_x - q_y)a/4]}{it(2q'_z + 3q_x - q_y)(2q'_z - q_x + 3q_y)} \left\{ \exp[i(q_y - q_x)e'] \right. \right. \\ & - \exp[i(q_y - q_x)e] \left(\cos[(2q'_z + q_x + q_y)e] \right. \\ & \left. \left. + \frac{2i(q_y - q_x) \sin[(2q'_z + q_x + q_y)e]}{(2q'_z + q_x + q_y)} \right) \right\} \\ & \left. + (\text{complex conjugate}) \right]. \quad (10) \end{aligned}$$

The corresponding contributions from $(2\bar{2}\bar{2})$ and $(\bar{2}22)$ triangular faces could easily be

written as follows by substituting $-q_y$ for q_y in (9) and (10):

$$\begin{aligned} \sigma_z(\bar{2}\bar{2}2) = & \left[\frac{4 \exp[i(tq_z + q_x - q_y)a/4]}{it(2q'_z - 3q_x - q_y)(2q'_z + q_x + 3q_y)} \left\{ \exp[-i(q_x + q_y)e'] \right. \right. \\ & - \exp[-i(q_x + q_y)e] \left(\cos[(2q'_z - q_x + q_y)e] \right. \\ & \left. \left. - \frac{2i(q_x + q_y) \sin[(2q'_z - q_x + q_y)e]}{(2q'_z - q_x + q_y)} \right) \right\} \\ & \left. + (\text{complex conjugate}) \right] \end{aligned} \quad (11)$$

and

$$\begin{aligned} \sigma_z(\bar{2}22) = & \left[\frac{4 \exp[i(tq_z - q_x + q_y)a/4]}{it(2q'_z + 3q_x + q_y)(2q'_z - q_x - 3q_y)} \left\{ \exp[-i(q_x + q_y)e'] \right. \right. \\ & - \exp[-i(q_x + q_y)e] \left(\cos[(2q'_z + q_x - q_y)e] \right. \\ & \left. \left. - \frac{2i(q_x + q_y) \sin[(2q'_z + q_x - q_y)e]}{(2q'_z + q_x - q_y)} \right) \right\} \\ & \left. + (\text{complex conjugate}) \right]. \end{aligned} \quad (12)$$

On the other hand, the co-ordinate axes transformation

$$Z = \sin \theta (tz/2 + x), \quad X = \cos \theta (x - 2z/t) \quad \text{and} \quad Y = y \quad (13)$$

rotates z and x axes through an angle $\theta = \tan^{-1}(2/t)$ about y axis and orients the (201) decagonal face perpendicular to Z axis. Its contribution is therefore given by

$$\begin{aligned} \sigma_z(201) = & \left[\frac{\exp[i(tq_z/2 + q_x)Z]}{i} \right]^{a/4} \\ & \times \int_{-e'}^{e'} \int_{-a'}^{a'} \exp[i(q_x - 2q'_z)X] \exp(iq_y Y) ds_z, \end{aligned} \quad (14)$$

where $a' = a(2 + t^2)/8$. This integral is evaluated to arrive at the expression

$$\begin{aligned} \sigma_z(201) = & \frac{4 \exp[i(tq_z + 2q_x)a/8]}{it} \left(\left\{ \cos(q_y a') - \cos \left[\frac{q_y a}{4} \right] \cos[(2q'_z - q_x)2e] \right. \right. \\ & \left. \left. + \left(\frac{2q'_z - q_x}{q_y} \right) \sin \left[\frac{q_y a}{4} \right] \sin[(2q'_z - q_x)2e] \right\} / \{(2q'_z - q_x)^2 - q_y^2\} \right. \\ & \left. + \left\{ 3 \left(\cos \left[\frac{q_y a}{4} \right] \cos[(2q'_z - q_x)2e] - \cos(q_y a') \cos[(2q'_z - q_x)e'] \right) \right. \right. \\ & \left. \left. - \left(\frac{2q'_z - q_x}{q_y} \right) \left(\sin \left[\frac{q_y a}{4} \right] \sin[(2q'_z - q_x)2e] \right) \right\} \right) \end{aligned}$$

$$-\sin(q_y d') \sin[(2q'_z - q_x)e'] \Big) \Big/ \left\{ (2q'_z - q_x)^2 - (3q_y)^2 \right\}. \quad (15)$$

The corresponding contributions from $(\bar{2}01)$, $(02\bar{1})$ and $(0\bar{2}\bar{1})$ decagonal faces could be expressed as follows by substituting $-q_x$ for q_x in (15), by interchanging $-q_x$ with q_y and $-q_y$ in the complex conjugate of (15):

$$\begin{aligned} \sigma_z(\bar{2}01) = & \frac{4\exp[i(tq_z - 2q_x)a/8]}{it} \left(\left\{ \cos(q_y a') - \cos\left[\frac{q_y a}{4}\right] \cos[(2q'_z + q_x)2e] \right. \right. \\ & + \left. \left. \left(\frac{2q'_z + q_x}{q_y}\right) \sin\left[\frac{q_y a}{4}\right] \sin[(2q'_z + q_x)2e] \right\} \Big/ \left\{ (2q'_z + q_x)^2 - q_y^2 \right\} \right. \\ & + \left\{ 3 \left(\cos\left[\frac{q_y a}{4}\right] \cos[(2q_z + q_x)2e] - \cos(q_y d') \cos[(2q'_z + q_x)e'] \right) \right. \\ & - \left. \left(\frac{2q'_z + q_x}{q_y}\right) \left(\sin\left[\frac{q_y a}{4}\right] \sin[(2q'_z + q_x)2e] \right. \right. \\ & \left. \left. - \sin(q_y d') \sin[(2q'_z + q_x)e'] \right) \right\} \Big/ \left\{ (2q'_z + q_x)^2 - (3q_y)^2 \right\} \Big), \quad (16) \end{aligned}$$

$$\begin{aligned} \sigma_z(02\bar{1}) = & \frac{4\exp[-i(tq_z - 2q_y)a/8]}{-it} \left(\left\{ \cos(q_x a') - \cos\left[\frac{q_x a}{4}\right] \cos[(2q'_z + q_y)2e] \right. \right. \\ & + \left. \left. \left(\frac{2q'_z + q_y}{q_x}\right) \sin\left[\frac{q_x a}{4}\right] \sin[(2q'_z + q_y)2e] \right\} \Big/ \left\{ (2q'_z + q_y)^2 - q_x^2 \right\} \right. \\ & + \left\{ 3 \left(\cos\left[\frac{q_x a}{4}\right] \cos[(2q'_z + q_y)2e] - \cos(q_x d') \cos[(2q'_z + q_y)e'] \right) \right. \\ & - \left. \left(\frac{2q'_z + q_y}{q_x}\right) \left(\sin\left[\frac{q_x a}{4}\right] \sin[(2q'_z + q_y)2e] \right. \right. \\ & \left. \left. - \sin(q_x d') \sin[(2q'_z + q_y)e'] \right) \right\} \Big/ \left\{ (2q'_z + q_y)^2 - (3q_x)^2 \right\} \Big) \quad (17) \end{aligned}$$

and

$$\begin{aligned} \sigma_z(0\bar{2}\bar{1}) = & \frac{4\exp[-i(tq_z + 2q_y)a/8]}{-it} \left(\left\{ \cos(q_x a') - \cos\left[\frac{q_x a}{4}\right] \cos[(2q'_z - q_y)2e] \right. \right. \\ & + \left. \left. \left(\frac{2q'_z - q_y}{q_x}\right) \sin\left[\frac{q_x a}{4}\right] \sin[(2q'_z - q_y)2e] \right\} \Big/ \left\{ (2q'_z - q_y)^2 - q_x^2 \right\} \right. \\ & + \left\{ 3 \left(\cos\left[\frac{q_x a}{4}\right] \cos[(2q'_z - q_y)2e] - \cos(q_x d') \cos[(2q'_z - q_y)e'] \right) \right. \\ & - \left. \left(\frac{2q'_z - q_y}{q_x}\right) \left(\sin\left[\frac{q_x a}{4}\right] \sin[(2q'_z - q_y)2e] \right. \right. \\ & \left. \left. - \sin(q_x d') \sin[(2q'_z - q_y)e'] \right) \right\} \Big/ \left\{ (2q'_z - q_y)^2 - (3q_x)^2 \right\} \Big). \quad (18) \end{aligned}$$

Making use of the co-ordinate axes transformation

$$Z = \sin \theta' (\frac{3}{2}tz + y), \quad X = x \quad \text{and} \quad Y = \cos \theta' (y - 2z/3t) \quad (19)$$

which rotates y and z axes through an angle $\theta' = \tan^{-1}(2/3t)$ about x axis and orients the (023) hexagonal face perpendicular to Z axis, its contribution to σ_z is expressed as

$$\begin{aligned} \sigma_z(023) &= \left[\frac{\exp \{ i(\frac{3}{2}tq_x + q_y)Z \}}{i} \right]^{a/4} \\ &\times \int_{-b'}^{b'} \int_{-e'}^{e'} \exp(iq_x X) \exp \{ i(q_y - 2q_z/3t)Y \} ds_z, \end{aligned} \quad (20)$$

where $b' = a(2 - t^2)/8$. The evaluation of this integral yields

$$\begin{aligned} \sigma_z(023) &= \left(\frac{4 \exp [i(3tq_x + 2q_y)a/8]}{it[(3q_y - 2q'_z)^2 - q_x^2]} \right) \\ &\times \left\{ \cos(q_x b') - \cos(q_x d') \cos[(3q_y - 2q'_z)e] \right. \\ &\left. + \left(\frac{3q_y - 2q'_z}{q_x} \right) \sin(q_x d') \sin[(3q_y - 2q'_z)e] \right\}. \end{aligned} \quad (21)$$

The corresponding contributions from $(0\bar{2}3)$, $(20\bar{3})$ and $(\bar{2}0\bar{3})$ hexagonal faces could be written as follows by substituting $-q_y$ for q_y in (21), by interchanging $-q_y$ respectively with q_x and $-q_x$ in the complex conjugate of (21):

$$\begin{aligned} \sigma_z(0\bar{2}3) &= \left(\frac{4 \exp [i(3tq_x - 2q_y)a/8]}{it[(3q_y + 2q'_z)^2 - q_x^2]} \right) \\ &\times \left\{ \cos(q_x b') - \cos(q_x d') \cos[(3q_y + 2q'_z)e] \right. \\ &\left. + \left(\frac{3q_y + 2q'_z}{q_x} \right) \sin(q_x d') \sin[(3q_y + 2q'_z)e] \right\}, \end{aligned} \quad (22)$$

$$\begin{aligned} \sigma_z(20\bar{3}) &= \left(\frac{4 \exp [-i(3tq_x - 2q_x)a/8]}{-it[(3q_x + 2q'_z)^2 - q_y^2]} \right) \\ &\times \left\{ \cos(q_y b') - \cos(q_y d') \cos[(3q_x + 2q'_z)e] \right. \\ &\left. + \left(\frac{3q_x + 2q'_z}{q_y} \right) \sin(q_y d') \sin[(3q_x + 2q'_z)e] \right\} \end{aligned} \quad (23)$$

and

$$\begin{aligned} \sigma_z(\bar{2}0\bar{3}) &= \left(\frac{4 \exp [-i(3tq_x + 2q_x)a/8]}{-it[(3q_x - 2q'_z)^2 - q_y^2]} \right) \\ &\times \left\{ \cos(q_y b') - \cos(q_y d') \cos[(3q_x - 2q'_z)e] \right\} \end{aligned}$$

$$+ \left(\frac{3q_x - 2q'_z}{q_y} \right) \sin(q_y d') \sin[(3q_x - 2q'_z)e] \} \quad (24)$$

Similar expressions for the contributions from triangular, decagonal and hexagonal faces to σ_x as well as σ_y are obtained by taking into account the differences in the corresponding components of area of these faces. For instance, the z component is t times the x or y component of area of (222) triangular faces and their contributions to the latter are therefore given by

$$\begin{aligned} & \sigma_x(222) + \sigma_x(\bar{2}\bar{2}2) + \sigma_x(2\bar{2}\bar{2}) + \sigma_x(\bar{2}2\bar{2}) \\ & = [\sigma_z(222) - \sigma_z(\bar{2}\bar{2}2) + \sigma_z(2\bar{2}\bar{2}) - \sigma_z(\bar{2}2\bar{2})]/t \end{aligned} \quad (25)$$

and

$$\begin{aligned} & \sigma_y(222) + \sigma_y(\bar{2}\bar{2}2) + \sigma_y(2\bar{2}\bar{2}) + \sigma_y(\bar{2}2\bar{2}) \\ & = [\sigma_z(222) - \sigma_z(\bar{2}\bar{2}2) - \sigma_z(2\bar{2}\bar{2}) + \sigma_z(\bar{2}2\bar{2})]/t. \end{aligned} \quad (26)$$

On the contrary, the x component or the y component is $(2/t)$ and $(2/3t)$ times the z component of area of the decagonal and hexagonal faces, respectively and hence their contributions to the former and the latter are related by

$$\sigma_x(201) + \sigma_x(\bar{2}0\bar{1}) = 2[\sigma_z(201) - \sigma_z(\bar{2}0\bar{1})]/t, \quad (27)$$

$$\sigma_y(02\bar{1}) + \sigma_y(0\bar{2}1) = -2[\sigma_z(02\bar{1}) - \sigma_z(0\bar{2}1)]/t, \quad (28)$$

$$\sigma_x(20\bar{3}) + \sigma_x(\bar{2}0\bar{3}) = -2[\sigma_z(20\bar{3}) - \sigma_z(\bar{2}0\bar{3})]/3t \quad (29)$$

and

$$\sigma_y(023) + \sigma_y(0\bar{2}3) = 2[\sigma_z(023) - \sigma_z(0\bar{2}3)]/3t. \quad (30)$$

3.3 Expressions for $S(\mathbf{q})$

It is possible to write down the interference factor for each of these polyhedra in two different forms by substituting the expressions for the components of σ in 2(a) and 2(b). Since the expressions so obtained for $S_2(\mathbf{q}, t)$ and $S_3(\mathbf{q}, t)$ consist of scalar terms, they could be reduced to convenient forms. In the case of atomic polyhedron for instance, the expression for $S_2(\mathbf{q}, t)$ reduces to (A-1) when the terms with common denominator are collected together while that for $S_3(\mathbf{q}, t)$ reduces to (A-2) when the products of the trigonometric functions are transformed into their sums and these are included in Appendix A. On the other hand, in the case of lattice polyhedron (which corresponds to the atomic polyhedron of monatomic bct lattice) the expression for $S_2(\mathbf{q}, t)$ goes over to (A-3) of I when the sums of the trigonometric functions are transformed into their products whereas the reverse transformation reduces that for $S_3(\mathbf{q}, t)$ to (A-4) of I, but

planes of the lattice polyhedron, the contributions from all faces, except a pair of square faces, to the interference factors of the atomic polyhedron become complex. However, the contributions from decagonal and hexagonal faces and those from square and triangular faces are not shown separately in (A-1) or (A-2) as the former could easily be distinguished from the latter in these expressions for $S(\mathbf{q}, t)$. Nevertheless, there is no simple and straightforward method of obtaining the interference factors of one polyhedron from those of the other.

Notwithstanding the apparent differences, it could be shown that the expressions for $S_2(\mathbf{q}, t)$ and $S_3(\mathbf{q}, t)$ reduce to the same expressions along the principal symmetry directions of the crystal provided L' Hospital's rule is made use of to overcome their singularities. These expressions for the interference factor of the atomic polyhedron along $[\zeta 00]$, $[\zeta \zeta 0]$ and $[00\zeta]$ directions, where ζ is the appropriate reduced wave vector, denoted respectively by (B-1), (B-2) and (B-3) are included in Appendix B. Corresponding expressions of the lattice polyhedron, denoted by (B-4), (B-5) and (B-6) are given in Appendix B of I. It may be observed that each of these expressions tends to unity in the limit of $\zeta \rightarrow 0$ and becomes zero whenever ζ corresponds to a reciprocal lattice vector, $\mathbf{g} \neq 0$. To demonstrate the basic differences between the two interference factors of white tin, they have been plotted as a function of ζ in figures 2(a), (b) and (c), respectively along $[\zeta 00]$, $[\zeta \zeta 0]$ and $[00\zeta]$ directions as well as in figure 2(d) along a non-symmetry direction $[\zeta \zeta 2\zeta]$. Numerical values of the interference factor, $G(qr_s)$ which approximates the atomic polyhedron as well as the lattice polyhedron by an ellipsoid of equivalent volume, calculated from the expression (C-1) in Appendix C (the definition of qr_s given in I is erroneous) have also been plotted in these figures to facilitate their comparison with the corresponding values of $S(\zeta, t)$.

4. Discussion

It is obvious from figures 2(a), (b), (c) and (d) that the interference factors, $S(\zeta, t)$ and $G(qr_s)$ vary considerably with the direction as well as the volume of the polyhedron and the former goes through zero at values of ζ corresponding to $\mathbf{g} \neq 0$, whereas the latter does not. Further, $S(\zeta, t)$ of the lattice polyhedron reduces to zero at all reciprocal lattice vectors of bct lattice with $t < 1$ while that of the atomic polyhedron becomes zero only at some of these vectors but not at others (see figure 2c). Thus an enlarged unit cell which generates these selected vectors but eliminates the rest, is compatible with the atomic polyhedron. In addition, $S(\zeta, t)$ of the former differs from that of the latter, even at small wave vectors, in all directions except $[00\zeta]$ direction and these differences are far more significant than the corresponding difference between $S(\zeta, t)$ and $G(qr_s)$ in the case of either polyhedron, precisely because the complex shape of the atomic polyhedron is closer to the ellipsoid of equivalent volume rather than to the shape of the lattice polyhedron. Nevertheless, the surface of the atomic polyhedron does not match with that of the ellipsoid of equivalent volume in any direction and the former lies inside the latter along $[\zeta 00]$, $[\zeta \zeta 0]$, $[00\zeta]$ and $[\zeta \zeta 2\zeta]$ directions. Consequently, the values of $S(\zeta, t)$ are lower than those of $G(qr_s)$ but the proximity of these surfaces gives rise to least difference between the two along $[\zeta \zeta 0]$ direction. In the case of lattice polyhedron, on the other hand, this difference is positive along $[00\zeta]$ and $[\zeta \zeta 2\zeta]$ directions while it is negative along $[\zeta 00]$ and $[\zeta \zeta 0]$ directions. Since the volume of the lattice polyhedron is

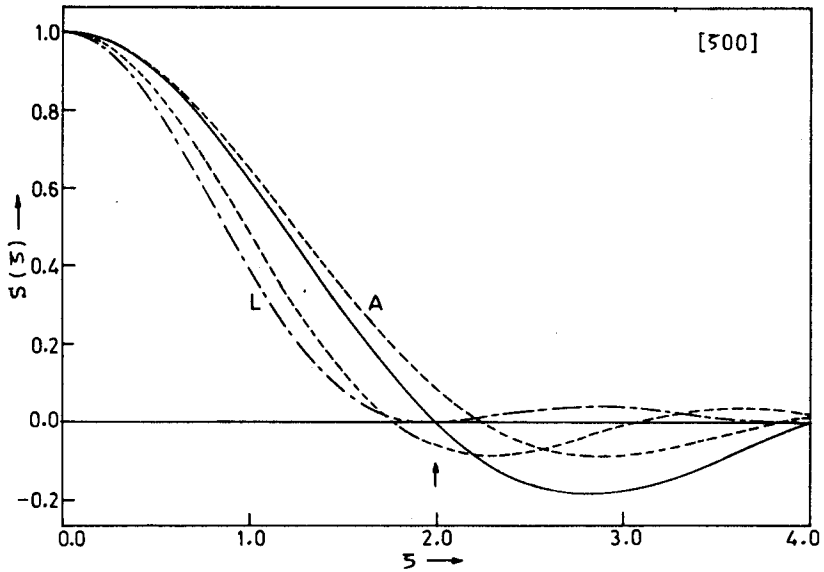
twice that of the atomic polyhedron, the corresponding difference between the $G(qr_s)$ or the matching of the ellipsoid surfaces is devoid of any significance.

It can be shown that the reciprocal lattice vectors associated with the atomic polyhedron of diatomic white tin, determined from the numerical values of ζ at which its $S(\zeta, t)$ goes through zero, correspond to a bct lattice with unit cell dimensions $4\pi/a$, $4\pi/a$ and $8\pi/c$ whereas those associated with the lattice polyhedron belong to a fct lattice with unit cell dimensions $4\pi/a$, $4\pi/a$ and $4\pi/c$. The axial ratio of the former is twice that of the latter, each being > 1 . However, the reciprocal lattice vectors deduced from the x-ray structure factors of bct white tin do not correspond to either of these lattices. In this context, it may be recalled that the interference factor, $S(\zeta, t)$ reduces to zero at a reciprocal lattice vector while the structure factor does not. Consequently, the former rejects a reciprocal lattice vector associated with the lattice polyhedron and the latter retains it when the contributions from the basis atoms fail to reduce both factors to zero. It should therefore be obvious from this discussion that the basis atoms have created some confusion regarding the correct shape and size of the first Brillouin zone in the case of white tin. For example, the size of the Brillouin zone associated with the atomic polyhedron and the lattice polyhedron, deduced respectively from the bct lattice and the fct lattice, are twice and half that deduced from the x-ray structure factors. The latter is a distorted dodecahedron of volume $32 \pi^3/a^2c$ which could accommodate all modes of vibration associated with a diatomic bct lattice. Nevertheless most lattice dynamical calculations on white tin (Brovman and Kagan 1966; Chen 1967; Kam and Gilat 1968) have made use of the Brillouin zone of a monatomic bct lattice with $t < 1$, which is identical with that of the lattice polyhedron. The additional modes of vibration due to basis atoms are taken into account by the optical branches in this reduced zone. On the contrary, the present investigations reveal that $S(\zeta, t)$ of the atomic polyhedron of white tin is not compatible with either of these zones.

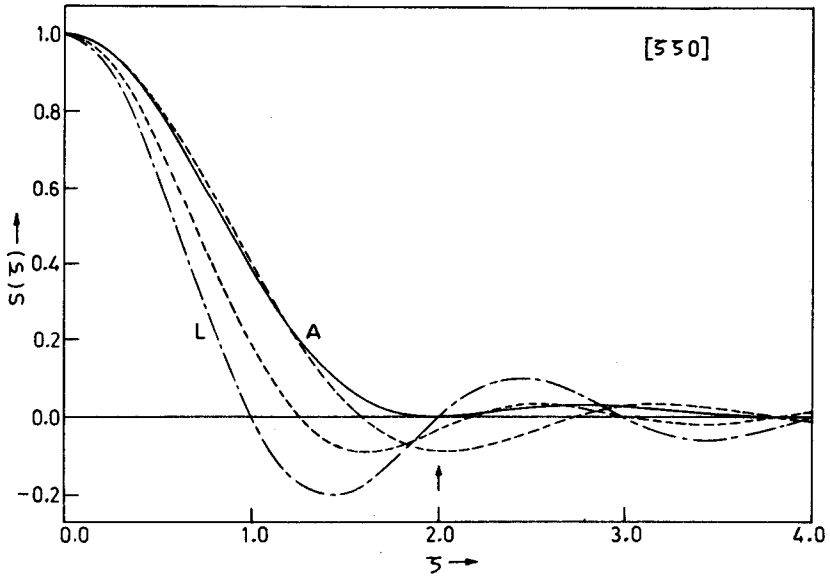
Since the atomic arrangement of diatomic bct tin is associated with two different polyhedra, the basic differences between the corresponding sets of reciprocal lattice vectors could be reconciled by associating all Brillouin zones with the same reciprocal lattice. For this purpose, we make use of the bct lattice compatible with the atomic polyhedron. All the reciprocal lattice vectors associated with the lattice polyhedron and those associated with x-ray structure factors are generated by this lattice with three basis vectors defined by

$$\mathbf{b}_1^* = \frac{2\pi}{a} [\hat{i} + \hat{j}], \quad \mathbf{b}_2^* = \frac{2\pi}{c} [t\hat{j} + \hat{k}] \quad \text{and} \quad \mathbf{b}_3^* = \frac{2\pi}{c} [t\hat{i} + \hat{k}] \quad (31)$$

and two basis vectors (\mathbf{b}_2^* and \mathbf{b}_3^*), respectively. It should therefore be clear from this representation that the basis atoms reduce the x-ray structure factors, corresponding to only one set of basis vectors, to zero even though their contributions to $S(\zeta, t)$ never become zero at any basis vector. Besides, the "atomic polyhedron" of this lattice which corresponds to the smallest of the three Brillouin zones, is linked with the lattice polyhedron while the "lattice polyhedron" of this lattice which corresponds to the largest of the three Brillouin zones, is linked with the atomic polyhedron of white tin. On the contrary, the "atomic polyhedron" of the bct lattice with only two basis points which is identical with the other Brillouin zone, is not connected with either polyhedron. In addition, it is necessary to recall from I that the diatomic bct lattice is derived from the diamond cubic lattice by exploiting the crystallographic equivalence between fct and bct lattices. The sp^3 hybridization doubles the size of the Brillouin zones to accommodate four electrons per atom in each zone. Nevertheless, the shape



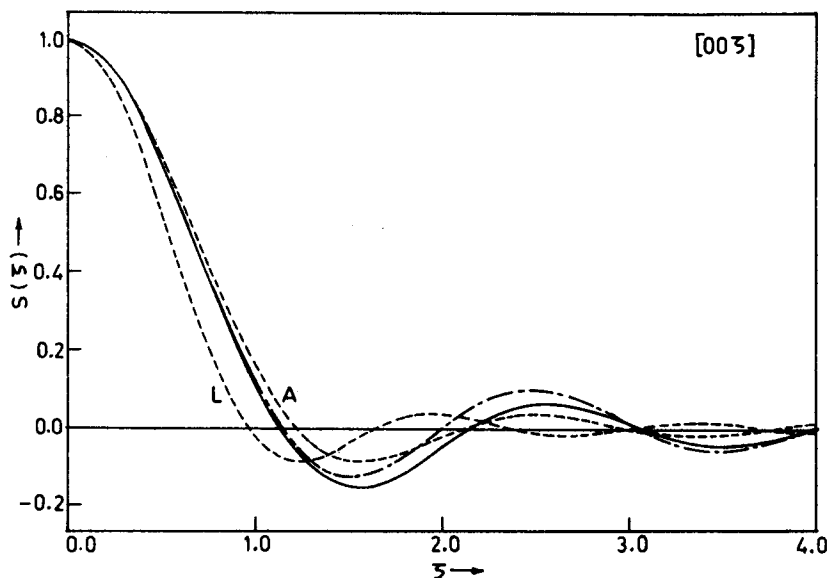
2(a)



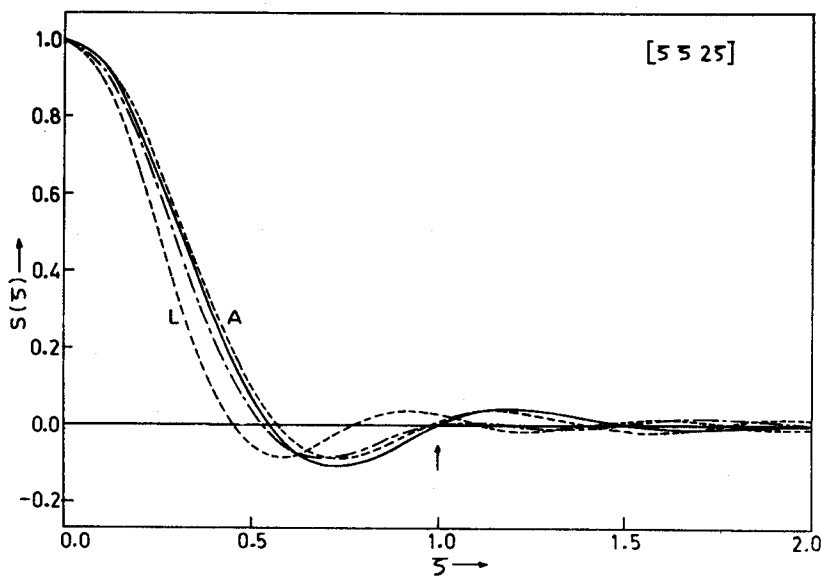
2(b)

and size of the first Brillouin zone for the electrons of white tin are identical with those of the "lattice polyhedron" (Mott and Jones 1936). The electron-phonon interactions should therefore be evaluated using $S(\zeta, t)$ of the atomic polyhedron and the reciprocal lattice vectors generated by the bct lattice.

It was shown in I that the Wigner-Seitz approximation leads to an erroneous



2(c)



2(d)

Figure 2. ζ -dependence of interference factors in the case of diatomic white tin along (a) $[\zeta 0 0]$ direction, (b) $[\zeta \zeta 0]$ direction, (c) $[0 0 \zeta]$ direction and (d) $[\zeta \zeta \zeta]$ direction (see Appendix for appropriate expressions); atomic polyhedron (A) $S(\zeta)$ —, $G(qr_s)$ —; lattice polyhedron (L) $S(\zeta)$ —, $G(qr_s)$ — . The arrows indicate that both $S(\zeta)$ pass through zero whereas either $G(qr_s)$ does not, at non-zero reciprocal lattice vectors. At $\zeta = 1.0$ and 3.0 in (b) as well as at $\zeta = 2.0$ in (c) $S(\zeta)$ of the latter reduces to zero but that of the former does not.

evaluation of the contributions from umklapp processes to the thermal and electrical properties of metals and is not consistent with the symmetry requirements of the lattice. Further, the acoustical and optical modes of vibration of a diatomic lattice are linked, respectively with the 'in-phase' and 'out of phase' motion of the basis atoms. Since the contributions from the basis atoms are completely ignored by $S(\zeta, t)$ of the lattice polyhedron, but are mixed up with those from lattice atoms in $G(qr_s)$ of the atomic polyhedron, evaluation of the electron-phonon interactions using either of these interference factors yields the same contributions to optical as well as acoustical modes of vibration and neither of these branches conforms to the translational symmetry of the lattice. Perhaps, this is one of the reasons for not incorporating the electron-phonon interactions into the lattice dynamical models for bct white tin (Wolfram *et al* 1963; De Wames and Lehman 1964; Brovman and Kagan 1966; Kam and Gilat 1968, Ramjirao and Narayanamurthy 1985). It should therefore be obvious from this discussion that the correct evaluation of the contributions from normal and umklapp processes to different modes of vibration in a diatomic lattice requires the exact evaluation of the interference factor over the actual shape of the atomic polyhedron so that it is expressed as a sum of contributions from basis planes (bisecting the basis vectors) and lattice planes (bisecting the lattice vectors). Lattice dynamical study of white tin based on an elastically consistent model which incorporates the electron-phonon interactions, for the first time, is described elsewhere (Rajendraprasad 1982).

5. Conclusions

The symmetry of the atomic polyhedron of diatomic white tin considerably simplifies the exact evaluation of electron-phonon matrix elements over its actual shape and facilitates the separation of the lattice atom contributions from the basis atom contributions to the interference factor $S(\mathbf{q}, t)$. Nevertheless, the expressions for $S(\mathbf{q}, t)$ of the lattice polyhedron which ignore the basis atom contributions entirely, cannot be derived from those of the atomic polyhedron. The reciprocal lattice vectors associated with the latter are quite different from those associated with the former. Since the lattice and basis plane contributions are inseparable in $G(qr_s)$, the Wigner-Seitz approximation is not valid for a diatomic lattice and exact expressions for $S(\mathbf{q}, t)$ of the atomic polyhedron together with a compatible set of reciprocal lattice vectors are required for a proper evaluation of the thermal and electrical properties of white tin and to satisfy the symmetry requirements of the lattice.

Acknowledgements

The author is grateful to Dr S B Rajendraprasad for many valuable and stimulating discussions and to Dr D Ranganathan and Mr A Thayumanavan for their assistance in computation.

Appendix A. Expressions for $S(\mathbf{q}, t)$ of the atomic polyhedron: general direction

$$\begin{aligned}
 S_2(\mathbf{q}, t) = & \left[\frac{2}{t^2(u+v+w)} \right] \left\{ [2t \sin(tw) \sin(\delta' u) \sin(\delta' v)/uv] + (t+2) \left[\frac{\exp[i(tw+u+v)/2]}{i(2w'-3u+v)(2w'+u-3v)} \right] \left(\exp[-i(u-v)\gamma'] \right. \right. \\
 & \left. \left. - \exp[-i(u-v)\epsilon/2] \right) \cos[(2w'-u-v)\epsilon/2] - 2i(u-v) \sin[(2w'-u-v)\epsilon/2]/(2w'-u-v) \right\} + \text{complex conjugate} \\
 & + t \left[\text{a term with } v \text{ and } -v \text{ interchanged} \right] + (t-2) \left[\frac{\exp[i(tw-u-v)/2]}{i(2w'+3u-v)(2w'-u+3v)} \right] \left(\exp[-i(u-v)\gamma'] - \exp[-i(u-v)\epsilon/2] \right) \\
 & \times \left\{ \cos[(2w'+u+v)\epsilon/2] - 2i(u-v) \sin[(2w'+u+v)\epsilon/2]/(2w'+u+v) \right\} + \text{complex conjugate} \left. \right] + t \left[\text{a term with } v \right. \\
 & \left. \text{and } -v \text{ interchanged} \right] + (t+2) \left[\exp[i(tw+2u)/4] \right] \left\{ \frac{\cos(\alpha v) - \cos[(2w'-u)\epsilon] \cos(v/2) - [(2w'-u)/v] \sin[(2w'-u)\epsilon] \sin(v/2)}{i[(2w'-u)^2 - v^2]} \right. \\
 & \left. + \frac{3(\cos[(2w'-u)\epsilon] \cos(v/2) - \cos[(2w'-u)\gamma'] \cos(\delta' v)) + [(2w'-u)/v] (\sin[(2w'-u)\gamma'] \sin(\delta' v) - \sin[(2w'-u)\epsilon] \sin(v/2))}{i[(2w'-u)^2 - (3v)^2]} \right\} \\
 & + (t-2) \left[\text{a term with } u \text{ and } -u \text{ interchanged} \right] + \text{two complex conjugate terms with } u \text{ and } v \text{ interchanged} \\
 & + (3t+2) \left[\exp[i(3tw+2v)/4] \right] \left\{ \frac{\cos(\beta u) - \cos[(2w'-3v)\epsilon/2] \cos(\delta' u) + [(2w'-3v)/u] \sin[(2w'-3v)\epsilon/2] \sin(\delta' u)}{i[(2w'-3v)^2 - u^2]} \right\} \\
 & \left. + (3t-2) \left[\text{a term with } v \text{ and } -v \text{ interchanged} \right] + \text{two complex conjugate terms with } u \text{ and } v \text{ interchanged} \right\} \quad (\text{A-1})
 \end{aligned}$$

$$\begin{aligned}
S_3(\mathbf{q}, t) = & \left[\frac{1}{t^2(u^2 + v^2 + w^2)} \right] \left\{ \left[t w \{ \sin(tw + \delta'u - \delta'v) + \sin(tw - \delta'u + \delta'v) - \sin(tw - \delta'u - \delta'v) \} / uv \right] \right. \\
& + \left[(tw + u + v) \left(\frac{\exp[i(tw + u + v)/2]}{i(2w' - u - v)} \right) \left\{ \frac{2(2w' - u - v)}{(2w' - 3u + v)} \exp[-i(u - v)\gamma'] - \frac{\exp[i(v - w')\epsilon]}{(2w' + u - 3v)} \right\} \right. \\
& \left. \left. + \text{complex conjugate} \right) \right] \\
& + \left[(tw - u - v) \left(\frac{\exp[i(tw - u - v)/2]}{i(2w' + u + v)} \right) \left\{ \frac{2(2w' + u + v)}{(2w' - u + 3v)} \exp[-i(u - v)\gamma'] - \frac{\exp[-i(w' + u)\epsilon]}{(2w' - u + 3v)} \right\} \right. \\
& \left. \left. + \text{complex conjugate} \right) \right] \\
& + \text{two additional terms with } v \text{ and } -v \text{ interchanged} \left. \right\} + \left[\frac{(tw + 2u) \exp[i(tw + 2u)/4]}{i} \right] \left\{ \frac{2 \cos(\alpha v)}{[(2w' - u)^2 - v^2]} \right. \\
& + \frac{2 \cos[(2w' - u)\epsilon + (v/2)]}{(2w' - u - 3v)} + \frac{2 \cos[(2w' - u)\gamma' + \delta'v]}{v(2w' - u - 3v)} + \frac{\cos[(2w' - u)\gamma' - \delta'v]}{v(2w' - u + 3v)} \left. \right\} \\
& + \text{a term with } u \text{ and } -u \text{ interchanged} + \text{two complex conjugate terms with } u \text{ and } v \text{ interchanged} \\
& + \left[\frac{(3tw + 2v) \exp[i(3tw + 2v)/4]}{i} \right] \left\{ \frac{2 \cos(\beta u)}{[(2w' - 3v)^2 - u^2]} - \frac{\cos(\epsilon w' - \gamma'v + \delta'u)}{u(2w' - 3v - u)} + \frac{\cos(\epsilon w' - \gamma'v - \delta'u)}{u(2w' - 3v + u)} \right\} \\
& + \text{a term with } v \text{ and } -v \text{ interchanged} + \text{two complex conjugate terms with } v \text{ and } u \text{ interchanged} \left. \right\} \quad (\text{A-2})
\end{aligned}$$

where $u = q_x a/2$, $v = q_y a/2$, $w = q_z a/2$, $w' = w/t$, $\epsilon = t^2/4$, $\alpha = (\frac{1}{2} + \epsilon)$, $\beta = (\frac{1}{2} - \epsilon)$, $\gamma' = \frac{3}{2}\epsilon$ and $\delta' = (1 - 3\epsilon)/2$.

Appendix B. Expressions for $S(\mathbf{q}, t)$ of the atomic polyhedron: symmetry directions

[ζ00] direction

$$S(\zeta, t) = \frac{32 \sin(\pi\zeta/2)}{9t^2(\pi\zeta)^3} \left[14 \sin^2\left(\frac{\gamma'\pi\zeta}{2}\right) - 12 \sin^2\left(\frac{\varepsilon\pi\zeta}{2}\right) + 6 \sin\left(\frac{5\varepsilon\pi\zeta}{4}\right) \sin\left(\frac{\varepsilon\pi\zeta}{4}\right) + (3\delta'\pi\zeta) \sin(\gamma'\pi\zeta) \right] \quad (\text{B-1})$$

[ζζ0] direction

$$S(\zeta, t) = \frac{2 \sin(\pi\zeta/2)}{t^2(\pi\zeta)^3} \left[3 \sin\left(\frac{\varepsilon\pi\zeta}{2}\right) \{2 \sin[(\beta + \gamma')\pi\zeta] - \sin[(\alpha - \gamma')\pi\zeta]\} + (2\varepsilon\pi\zeta) \sin(\alpha\pi\zeta) + \sin(\gamma'\pi\zeta) \sin(\delta'\pi\zeta) + \sin(\beta\pi\zeta) \sin(2\varepsilon\pi\zeta) + \sin(\varepsilon\pi\zeta) \sin\left(\frac{\pi\zeta}{2}\right) \right] \quad (\text{B-2})$$

[00ζ] direction

$$S(\zeta, t) = \frac{4t^4}{(\pi\zeta)^3} \left[\sin\left(\frac{\pi\zeta}{4}\right) \left\{ \sin^2\left(\frac{\pi\zeta}{4}\right) + 3 \sin\left(\frac{5\pi\zeta}{8}\right) \sin\left(\frac{\pi\zeta}{8}\right) + \left(\frac{\delta'\pi\zeta}{\varepsilon}\right) \sin\left(\frac{3\pi\zeta}{4}\right) \right\} + \sin^2\left(\frac{\pi\zeta}{8}\right) \left\{ 4 \sin\left(\frac{\pi\zeta}{2}\right) + 3 \sin\left(\frac{3\pi\zeta}{4}\right) \right\} \right] + \frac{4(\delta')^2 \sin(\pi\zeta)}{(\pi\zeta)} \quad (\text{B-3})$$

where the reduced wave vector, $\zeta = q_x a/2\pi$, $q_y a/2\pi$ and $q_z c/2\pi$ along x , y and z directions, respectively.

Appendix C. Expression for $G(qr_s)$

$$G(qr_s) = [3 \sin(qr_s) - (qr_s) \cos(qr_s)] / (qr_s)^3$$

where $qr_s = \left(\frac{6t}{\pi v}\right)^{1/3} [u^2 + v^2 + w^2]^{1/2}$ (C-1)

and v is the number of atoms per unit cell.

References

- Ashokkumar 1973 *Noncentral interactions in metals*. Ph.D. Thesis, Indian Institute of Technology, Delhi, p. 49
 Bross H and Bohn B 1967 *Phys. Status Solidi* **20** 277
 Brovman E G and Kagan Y U 1966 *Sov. Phys.—Solid State* **8** 1120
 Chen S H 1967 *Phys. Rev.* **163** 532
 De Wames R E and Lehman G W 1964 *Phys. Rev.* **135** A170
 Kam Z and Gilat G 1968 *Phys. Rev.* **175** 1156

- Mott N F and Jones H 1936 *The theory of the properties of metals and alloys* (Oxford: University Press) p.159
- Rajendraprasad S B 1982 *Lattice dynamical study of tetragonal metals*, Ph.D. Thesis, Indian Institute of Technology, Delhi, p. 132
- Ramamurthy V 1978 *Pramana (J. Phys.)* **11** 233
- Ramamurthy V 1979 *Pramana (J. Phys.)* **13** 373
- Ramamurthy V 1985 *Pramana (J. Phys.)* **24** 757
- Ramamurthy V and Rajendraprasad S B 1982 *Pramana (J. Phys.)* **19** 435
- Ramjirao R and Narayanamurthy J V S S 1985 *Indian J. Pure Appl. Phys.* **23** 16
- Sharan B, Ashokkumar and Neelakandan K 1973 *J. Phys.* **F3** 1308
- Wilson A H 1954 *Theory of metals* (Cambridge: University Press) p. 75
- Wolfram T, Lehman G W and De Wames R E 1963 *Phys. Rev.* **129** 2483